JOURNAL OF MATERIALS SCIENCE **37** (2002) 4227–4233

Analysis of crack development during processing of laminated ceramic tubes

Z. LIANG, S. BLACKBURN
IRC in Materials Processing and Department of Chemical Engineering, School of Engineering, The University of Birmingham, Edgbaston, Birmingham B15 2TT, UK
E-mail: S.Blackburn@bham.ac.uk

Models for the strain energy release rate in crack extension and tunnelling are taken from the literature with minor modification to take account of the compressive stresses in multi-layer ceramic tubes or composites. These models are applied to predict the potential for crack development in co-extruded tubes fabricated from combinations of alumina, zirconia (fully and partially stabilized) and zirconia toughened alumina. Experimental results show that the models predict the failure in the composites closely and thus form useful tools in the design of such structures. The main aspect of the predictive capacity is in the selection of the layer numbers and the layer thicknesses to prevent failure. The significance of crack-free layers is improved mechanical properties, in particular strength, and potential improvement in fracture toughness and device performance.

1. Introduction

Thin walled ceramic tubes are finding applications in many functional areas including fuel cells. These tubes require structural integrity and in the case of micro-reactors comprise layered materials, which facilitate the required functionality and structural integrity. Purely structural applications for thin-walled, multi-layered tubes are less common, but of increasing interest.

The potential of laminated ceramics to show superior properties was first demonstrated by Gutshall and Gross [1]. The toughness was shown to improve by placing the surfaces into residual compression, resulting in either an increase in intrinsic resistance to crack extension or a reduction of the crack driving force. In a series of papers by Clegg *et al*. [2, 3] it was shown that ceramic laminates could be toughened by the incorporation of weak interfaces giving rise to crack deflection. The optimum layer structure and compositions have been widely discussed. For example Russo *et al*. [4] designed a tri-layer composite consisting of two strong homogeneous outer layers and a more flow tolerant inner layer. This gave a 35% increase in strength over samples made only of the outer layer material. Marshall *et al*. [5] predicted that in a Ce-TZP/Al_2O_3 composite the Ce-TZP layers should be 20–200 μm in thickness to optimize toughness and produced a laminated structure with layers of Al_2O_3 separating Ce-TZP. The toughness increased from 5 MPam$^{0.5}$ to 17.5 MPam$^{0.5}$. Lakshminarayanan and Shetty [6] examined the effects of microscopic residual stresses on fracture toughness in multi-layer laminates, both analytically and experimentally. They produced a tri-layer composite with alumina +5% unstabilized zirconia as the outer layers and a central core of alumina +15 vol% fully stabilized zirconia placing the surfaces in residual compression, increasing the apparent toughness ~5 fold. Further, properties are enhanced by minimising the layer thickness, but it would be advantageous to be able to predict these optima.

The main problem with the preparation of ceramic laminates in tubular or sheet form is a propensity for cracking during processing, especially during the drying and sintering stages of their manufacture. In laminates where each layer is composed of a different material, which dries and sinters at a different rate than the adjacent layers, stresses develop in the individual layers depending on whether the adjacent layers are contracting or expanding relative to the layer under consideration. If these stresses exceed some critical value the layers will fail weakening the composite.

The drying process in ceramic materials can be complex and the linear shrinkage of the materials can be affected by the process and the morphology of the powders involved. In extrusion, particularly where the powders are highly concentrated in the binder, the linear shrinkage during drying is often small. In the work reported here, the linear shrinkages proved to be similar for all compositions, ~1%. In some laminates the layers vary only in dopant content and so such uniform shrinkage behaviour is to be expected. The majority of the differential shrinkage occurs during the sintering stage. In recent work on chocolate [7] cracking in composites is reported during extrusion, but in ceramic co-extrusion the paste flow characteristics (rheometry) are generally engineered to be similar [8] and thus cracking during the extrusion process was felt to be an unlikely occurrence. The authors had no visual evidence of its presence in the extrudates produced in the preparation of this work.

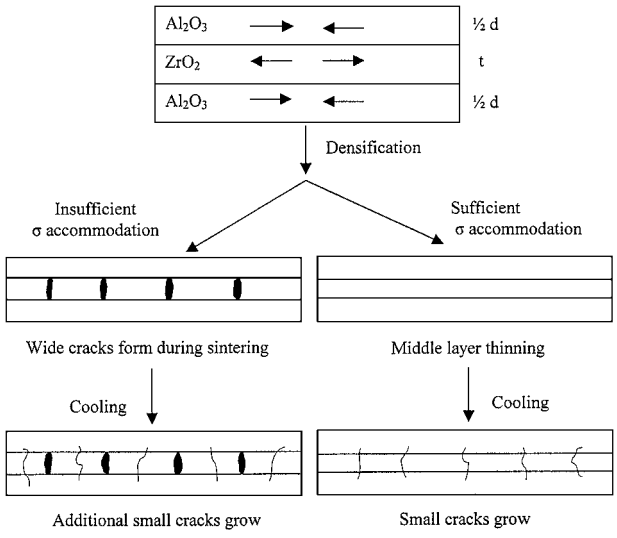

Figure 1 Schematic diagram illustrating the types of cracks which can develop during the sintering process.

Ceramics frequently sinter at different rates and to a different degree depending on their composition. However, the ability of the laminated composite to resist fracture during the sintering process will depend on the compliance of the layers. If at the sintering stage all the materials are compliant, rearrangement within the layers and accommodation of the imposed stresses are possible. The material will essentially be crack-free as it transfers from compliant to incompliant behaviour during cooling. When the layers exhibit reduced compliance, any differential sintering stresses will be accommodated by the development of cracks. Cracks that form at or close to the sintering temperatures of the laminate, will tend to be open and show signs of post fracture smoothing due to sintering. Further cracking may occur during cooling below the temperature marking the onset of brittle failure, if the thermal expansion coefficients of the layers are different. These cracks would tend to be less open and show brittle fracture surfaces. The above fracture modes are shown schematically in Fig. 1.

Experimental evidence suggests that cracking occurred largely at low temperatures in the brittle region. This implies that the process is controlled by the layer structure and the thermal expansion behaviour of the materials from which the laminate is constructed. In this paper, this hypothesis is explored by extending analyses developed by Ho *et al*. [9] and Hillman *et al*. [10] and verifying the results using thinwalled tubes prepared by a co-extrusion route.

2. Crack development analysis

In a composite comprising three layers (A, B, A), as shown in Fig. 2, the centre layer (B) will be placed under a tensile stress, if the shrinkage of B is greater than A. Thus a force balance exists, if the material is not failing, such that

$$\sigma_{(A)}t + \sigma_{(B)}d = 0 \tag{1}$$

where $\sigma_{(A)}$ and $\sigma_{(B)}$ are the normal stresses in layer A and B, respectively, t is the thickness of layer A and d is the thickness of layer B. In this situation $\varepsilon_0 = \varepsilon_A + \varepsilon_B$, where ε_0 is the residual strain in the system. Thus, Equation 1 can be written in terms of strain as

$$\frac{\varepsilon_A E_A t}{1-\nu_A} + \frac{\varepsilon_B E_B d}{1-\nu_B} = 0, \tag{2}$$

where ε_A and ε_B are the strain, E_A and E_B are Young's moduli and ν_A and ν_B are the Poisson's ratios of layers A and B respectively. The difference in the strain $\Delta\varepsilon_0$ is given by

$$\Delta\varepsilon_0 = \int_{T_i}^{T_f} (\alpha_A - \alpha_B)\,\mathrm{d}T \tag{3}$$

where α_A and α_B are the coefficients of thermal expansion (CTE) for layers A and B, respectively, and T_f and T_i are the final and initial temperatures. The initial temperature in this case was taken as the temperature marking the onset of brittle fracture. Here a value of 1200°C was chosen based on the work of Hillman *et al*. [10], cooling to a final temperature close to room temperature (25°C). Taking alumina (Al_2O_3) and zirconia with 3 mol% Yttria (ZrO_2(3Y)) as examples, data for the Young's moduli, μ, was found from the literature as 390 and 200 GPa respectively [11]. Poisson's ratio for both materials was assumed to be 0.27. Ho and Suo's study [9] confirmed that this assumption will influence the results only slightly. The CTE values were measured using a dilatometer (the method and results are given later) and the results for Al_2O_3 and ZrO_2(3Y) are shown in Fig. 3, as well as results for a zirconia toughened alumina containing 20% ZrO_2 and 80% Al_2O_3 (ZTA) and a zirconia with 8 mol% yttria (ZrO_2(Y8)). The values of CTE reported here for Al_2O_3 differ from those reported by Hillman *et al*. in form, but the mean values in the equations are similar and thus will not influence the results greatly.

The results for residual stress in an Al_2O_3/ZrO_2(3Y) tri-layer composite are shown in Fig. 4. The

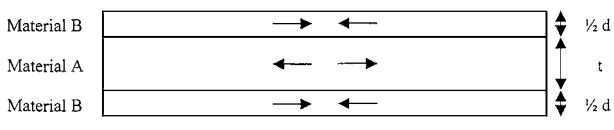

Figure 2 Schematic diagram illustrating the stress distribution in a trilayer laminate.

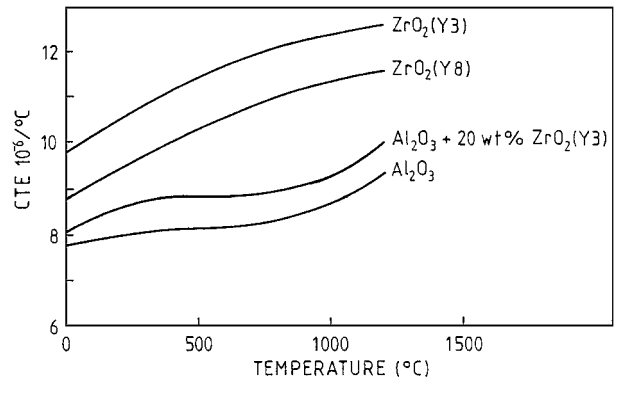

Figure 3 Coefficients of thermal expansion CTE (10^{-6}/°C) measured as a function of temperature for ZrO_2(Y3), ZrO_2(Y8), Al_2O_3 and Al_2O_3 + 20 wt% ZrO_2(Y3).

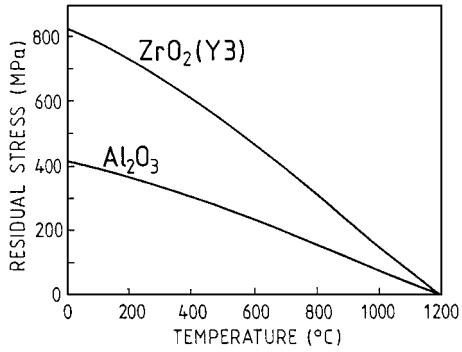

Figure 4 Calculated residual stresses as a function of temperature for the individual layers in an $Al_2O_3/ZrO_2(Y3)$ tri-layer tube, where Al_2O_3 is in compression and $ZrO_2(Y3)$ is in tension.

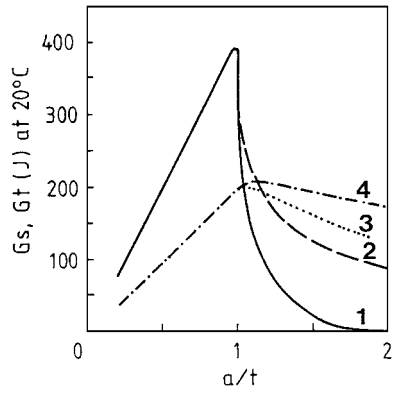

Figure 5 G_S and G_T as a function of a/t for an $Al_2O_3/ZrO_2(Y3)$ tri-layer tube with an even layer thickness ($t = 80$ μm) at 20°C. (1) G_S (present study), (2) G_S (Hillman *et al.* [10]), (3) G_T (present study), (4) G_T (Hillman *et al.* [10]).

compressive stress in the alumina reaches 409 MPa at 25°C, while the tensile stress in the $ZrO_2(3Y)$ layers reaches 818 MPa, these values being affected by the value selected for T_i, being larger of course if T_i is raised. Note that due to the alumina layers being half the thickness of the zirconia layers, the force balance given in Equation 1 is satisfied. Therefore the residual strain and stress as a function of temperature can be calculated.

Ho and Suo [9] developed a strain energy release rate expression of a crack present in a layer subject to biaxial tension. Hillman [10] modified Ho's analysis to take into account the crack extension into adjacent layers. From Fig. 1 it can be seen that as laminated materials cool from an initial temperature T_i, a tensile stress develops in the layers with the greatest contraction. When that tensile stress becomes sufficiently large, pre-existing flaws within the tensile layer will be subject to tension and may extend firstly through the layer and then into the adjacent compressive layers. Continued extension by tunnelling the crack along the interface is also possible. The energy release rates for both extending, G_S, and tunnelling, G_T, are the driving forces for crack extension in laminates on cooling. The strain energy release rate (G_S) subjected to tension (σ_1) and constrained by adjacent layers containing a compressive stress (σ_2) is given for the normalized crack length a/t by

$$G_S = \left(\frac{\pi}{2}\right)\frac{\sigma_1^2}{E_1^*}\left(\frac{a}{t}\right)t \qquad a/t < 1 \qquad (4)$$

and

$$G_S = \frac{\pi}{2}\frac{\sigma_1^2}{E_1^*}\left(\frac{a}{t}\right)\left[\sin^{-1}\left(\frac{t}{a}\right)\right]^2 t \qquad a/t > 1 \qquad (5)$$

For a given residual stress there is a critical layer thickness below which no cracks will extend regardless of internal flaw size. In the studies, compressive stress in the outer layers caused by the shrinkage of the middle layer was not taken into account. In this work, following the concepts of Watkins and Green [12], Hillman *et al.*'s analysis is further modified to take account of the compressive residual stresses in layers with higher CTEs. This brings about a modification to Equation 5 to give

$$G_S = \left(\frac{2}{\pi}\right)\frac{t}{E_1^*}\left(\frac{a}{t}\right)\left[\sigma_1 \sin^{-1}\left(\frac{t}{a}\right) - \sigma_2 \cos^{-1}\left(\frac{t}{a}\right)\right]^2 \qquad a/t > 1 \qquad (6)$$

where $E_1^* = E_A/(1-\mu_A^2)$ and a is the flaw size. The result of the analysis will be compared to those of Hillman and experiments have been conducted to evaluate the behaviour of real systems and the applicability of the model.

Fig. 5 plots G_S as a function of the normalized crack length, a/t, at 20°C for the composite with even layer thicknesses of 80 μm. When the crack is within the tensile layer, then there is no influence of the compressive layer and so for values of a/t below 1 the result follows Hillman *et al.*'s analysis. When the crack extends into the compressive layer ($a/t > 1$), the tensile stress quickly vanishes as the compressive stress works against growth.

The energy release rate (G_T), that drives the crack to extend along the layer (tunnelling), is given by Hillman *et al.* [10] as

$$G_T = \frac{1}{a}\int_0^a G_S(a)\,\mathrm{d}a \qquad (7)$$

By substituting Equations 4 and 5 into Equation 7 and solving the integral numerically, plots for the behaviour of G_T over a range of a/t values can be obtained. The results at 20°C are plotted in Fig. 5. Again the additional term influences the behaviour in the compressive layers, but note that the maximum value of G_T occurs when a/t is slightly above 1, where $G_S = G_T$ as was the case in Hillman *et al.*

Since both tensile (σ_1) and compressive (σ_2) stresses are functions of temperature, G_S and G_T will increase at higher temperature differences in accordance with Equations 4, 5 and 7. Fig. 6 plots G_S at different temperatures for an $Al_2O_3/ZrO_2(Y3)$ tri-layer composite with even layer thicknesses of 80 μm. As temperature is reduced from T_i, G_S increases.

Ho and Suo [9] show that a crack will not extend until the energy release rate reaches a critical value

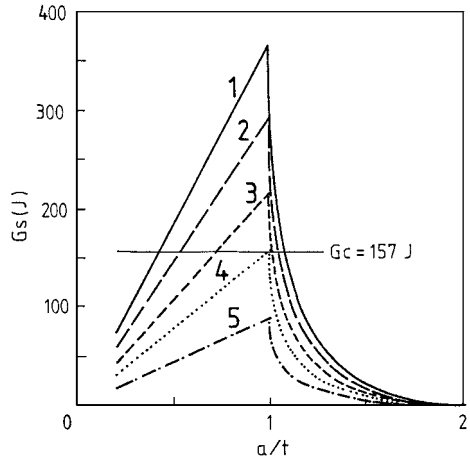

Figure 6 G_S as a function of a/t and temperature for an Al_2O_3/ZrO_2(Y3) tri-layer tube with an even layer thickness ($t = 80$ μm). G_C has the value of 157 J. G_S is shown at different temperatures, (1) 20°C, (2) 200°C (where $G_C = G_T$), (3) 400°C, (4) 530°C (where $G_C = G_S$) and (5) 700°C.

(G_C). This crack criterion is satisfied when

$$G_C < G_S \text{ or } G_T \tag{8}$$

G_C was estimated from the toughness (K_{1C}) of the tensile layer in the material using the expression

$$G_C = \frac{K_{iC}^2}{E_1}(1 - \nu^2) = \frac{K_{iC}^2}{E_i^*} \tag{9}$$

where K_{1C} is the measure of the ability of the material to resist fracture when a crack is present. K_{1C} was estimated by Vickers indentations using the equations proposed by Liang *et al.* [11]. This and other methods [13] for determining K_{1C} from indentations are known to overestimate the value. Thus, as K_{1C} appears in Equation 9, it is probable that G_C is overestimated to some degree.

The above analysis suggests that, if G_S and G_T can be controlled to be always smaller than G_C throughout the cooling process, a crack-free product should result, i.e., if $G_C > G_{S(max)}$ and $G_{T(max)}$, where $G_{S(max)}$ is the maximum value of G_S and $G_{T(max)}$ that of G_T. Both $G_{S(max)}$ and $G_{T(max)}$ are a function of the tensile layer thickness, t, and the maximum tensile stress ($\sigma_{1\,max}$) built up in the tensile layer during the whole cooling process. Thus following Hillman *et al.* [10]:

$$G_{S(max)} = \frac{\pi}{2}\frac{\sigma_{1\,max}^2}{E_1^*}t \tag{10}$$

and

$$G_{T(max)} = \frac{\pi}{4}\frac{\sigma_{1\,max}^2}{E_1^*}t \tag{11}$$

Since $G_{S(max)}$ is always greater than $G_{T(max)}$, the expression for crack-free densification can be simplified to

$$G_C > G_{S(max)} \tag{12}$$

Tensile stress is dependent on the ratio of the layer thicknesses, (d/t), the tensile layer thickness (t) and the difference between CTE values of the compressive and tensile layers, ($\alpha_1 - \alpha_2$). Thus the maximum tensile stress $\sigma_{1\,max}$ is given by

$$\sigma_{1\,max} = \frac{E_1 E_2 \int_{1200}^{T_{max-min}} (\alpha_1 - \alpha_2)\,dT}{(1 - \mu)(E_1 t/d + E_2)} \tag{13}$$

T_{min} can be determined by plotting the tensile stress against temperature. In the case of composites comprising layers of Al_2O_3 and ZrO_2(Y3) T_{min} occurs at room temperature. Equations 10, 12 and 13 suggest that by adjusting d/t, t and ($\alpha_1 - \alpha_2$), it is possible to reduce the probability of crack propagation and ultimately eliminate cracks growing prematurely in laminates during cooling from the sintering temperature.

The critical layer thickness, t_c, required to prevent the development of cracks can be derived from Equations 10 applying the criterion given in Equation 12, such that:

$$t_c = \frac{2}{\pi}\frac{G_C E_1^*}{\sigma_{1\,max}} \tag{14}$$

If the tensile layer thickness is fixed along with ($\alpha_1 - \alpha_2$), the influence of d/t with respect to G_S/t can be calculated. G_S increases with increasing d/t values, which implies that lower values of d/t should result in lower crack populations. This relationship is shown graphically for a Al_2O_3/ZrO_2(Y3) system with three layers in Fig. 7. The critical value of d/t, $(d/t)_c$, is determined from the intercept of $G_{S\,max}/t$ and G_C/t, which can be calculated as

$$\left(\frac{d}{t}\right)_c = \frac{E_1}{E_2}\frac{C}{E_1 - C} \tag{15}$$

where

$$C = \frac{1 - \mu}{\varepsilon}\sqrt{\frac{2G_C E_1}{\pi t(1 - \nu^2)}} \tag{16}$$

for tri-layer tubes. Thus, if d/t was below 0.5 with zirconia being the centre layer, Fig. 7 would predict that cracks would not be found.

If the dimensions, layer number and ($\alpha_1 - \alpha_2$) are fixed, then the tensile layer should be designed to be either very thin to reduce t or they should be much thicker to reduce σ_1 relative to the compressive layer.

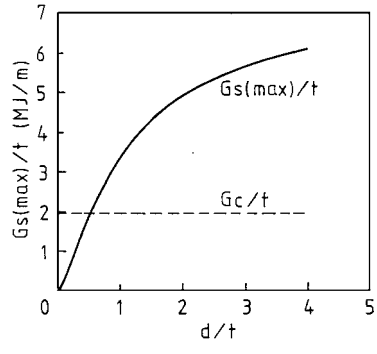

Figure 7 $G_{S(max)}$ as a function of d/t when $t = 80$ μm and $n = 3$ for Al_2O_3/ZrO_2(Y3) tubes.

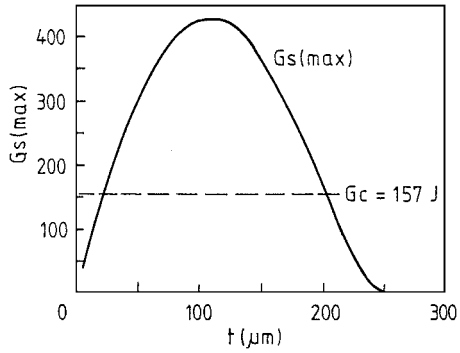

Figure 8 $G_{S(max)}$ as a function of t when $t + d = 250$ μm and $n = 3$ for $Al_2O_3/ZrO_2(Y3)$ tubes.

Fig. 8 shows G_S as a function of t for $Al_2O_3/ZrO_2(Y3)$ laminates ($n = 3$). Two critical values exist, where G_C crosses G_S. For the values of G_S to be small, the values of t must be either very small or very large. Hence, cracking should be observed between the two critical values of t.

Reducing $(\alpha_1 - \alpha_2)$ will reduce the tendency for crack propagation during cooling. In addition, the flaw size present in the processed ceramic will strongly influence the tendency for propagation. As shown in Fig. 5, where G_S and G_C are plotted against a/t, smaller defects are preferred to minimise crack growth potential. There exists a critical flaw size (a_c), which is given by

$$a_c = \frac{2}{\pi} \frac{G_C E_1^*}{\sigma_{1\,max}^2} \tag{17}$$

where

$$a_c = t_c/\sigma_{1\,max} \tag{18}$$

3. Experimental procedure

The preceding analysis was validated using a co-extrusion route with four paste compositions. The materials were formed using methods described by Alford *et al.* [14, 15] and a PVB based binder system. The powders were alumina [BAX 541, Alcan Chemicals], fully stabilized zirconia ($ZrO_2(Y8)$) [HSY8, Mandoval] and partially stabilized zirconia ($ZrO_2(Y3)$) [HSY3, Mandoval]. A ZTA was formed from 20 vol% of $ZrO_2(Y3)$ in Al_2O_3. This method of preparation produced thin sheets (approximately 1 mm thick), which were plastic in nature and could be cut and stacked in any desired combination for co-processing in the manner of van Hoy *et al.* [16]. Thin-walled tubes were made using a simple ram extruder in which a mandrel was supported on the end of the ram. The barrel was 20 mm in diameter and the die and mandrel were 3 mm and 2.3 mm in diameter respectively. The assembly was manufactured to our design and driven by a universal load frame (Instron 4467). The formulated sheets were wrapped around a central pin (2.3 mm in diameter), placed in the barrel and extruded through the die, yielding tube extrudates with an outside diameter of around 2.4 mm (after sintering) and 250 μm wall thickness [8]. For the best production of discrete, well defined layers the rheological properties of the pastes had to be similar. In this work a simple approach was adopted to verify the similarity of the pastes. When the load vs. ram speed plots were near coincident ($\pm 5\%$), then good co-extruded products resulted. Materials with up to 18 layers across the wall thickness were extrudable by this route. Thus, materials with a range of layer numbers, n, with various d, t, a/t, $\alpha_1 - \alpha_2$ combinations could be produced to evaluate the analysis. The extruded materials were dried at room temperature and then sintered at 1550°C for 1 hour in all cases.

The quality of the structures was examined in two ways. First, images of polished sections of the materials were taken using SEM analysis and the defect population observed qualitatively. Second, test specimens were subjected to three-point-bend analysis. The tube strength, σ_f, is given by

$$\sigma_f = \frac{FLR}{\pi(R^4 - r^4)} \tag{19}$$

where F is the load required to break the specimen, L is the span length, R is the outer diameter and r is the inner diameter of the tube.

In order to relate the experimental results to the theoretical analysis certain physical parameters had to be measured. Coefficients of thermal expansion were measured using a dilatometer (Netzsch 402 E) with sintered monolithic rods of the layer materials. Dilatometry was also used to assess the sintering characteristics of the materials in terms of linear shrinkage.

4. Results and discussion

Multi-layer tubes could be formed from combinations of the four paste formulations with layer numbers from $n = 1$ to 18. Three composite combinations were evaluated $ZrO_2(Y8)/Al_2O_3$, $ZrO_2(Y3)/Al_2O_3$ and ZTA/Al_2O_3. Equations 12 to 16 predict that the $ZrO_2(Y8)/Al_2O_3$ composites would be prone to failure. More than 18 layers would be required to prevent tensile layer crack growth, if the layers were of uniform thickness. Fig. 9 shows a co-processed $ZrO_2(Y8)/Al_2O_3$ composite with 11 layers in a thicker walled tube. The cracking in the tensile layers is clear. Given that the openings are both large and small, failure in this case may be a combination of differential sintering as well as cooling cracking. Reasons for the failure include the low strength and K_{1C} of $ZrO_2(Y8)$ relative to Al_2O_3. In tri-layer tubes, $n = 3$, the analysis predicted that d/t would need to be below 0.2 when t is 80 μm, giving a total wall thickness of 100 μm. Such a geometry was not attainable and the prediction could not be tested. In the systems available, where $d + t = 250$ μm and $n = 3$, t must be either below 10 μm or above 240 μm. To produce bodies with such geometries proved impractical due to failure of the layers through a form of boudinage (a term used in geology derived from the French for sausage where incompliant layers fail under elongation into rounded blocks [17]). All manufacturable geometries were predicted to fail and this proved to be the case.

The $ZrO_2(Y3)/Al_2O_3$ system proved more interesting, as the K_{1C} of the zirconia layers was, of course,

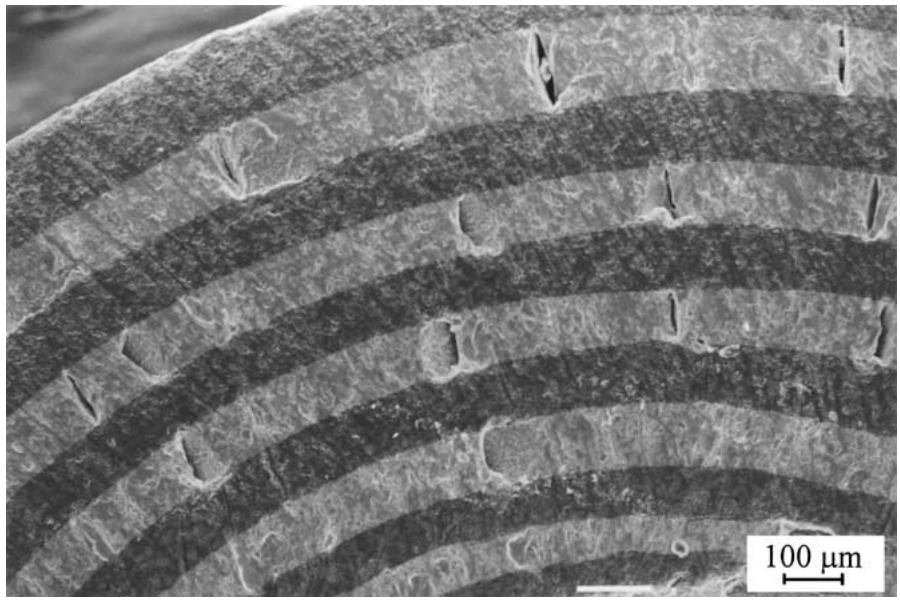

Figure 9 Cracks observed in an $Al_2O_3/ZrO_2(Y8)$ tube with 11 layers (wall thickness 900 μm).

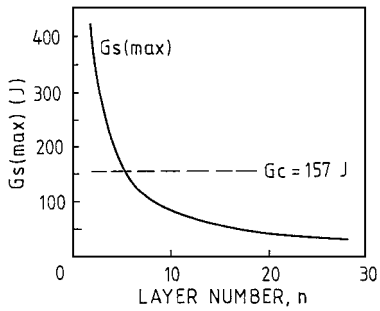

Figure 10 $G_{S(max)}$ as a function of layer number in $Al_2O_3/ZrO_2(Y3)$ tubes with 250 μm wall thickness and $d/t = 1$.

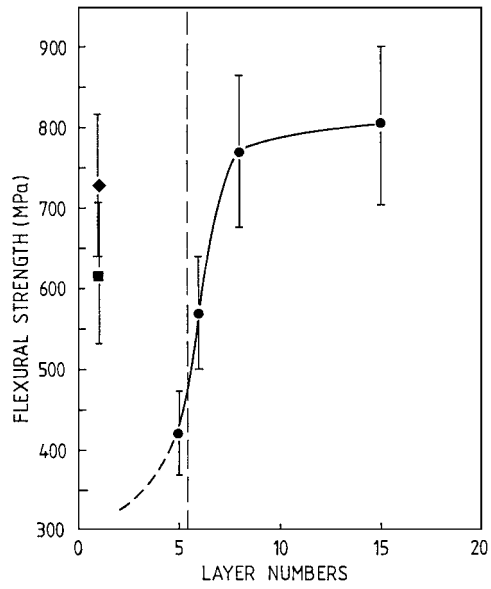

Figure 11 Flexural strength as a function of layer number in $Al_2O_3/ZrO_2(Y3)$ tubes with 250 μm wall thickness and $d/t = 1$, for (●) composites, (♦) $ZrO_2(Y3)$ and (■) Al_2O_3.

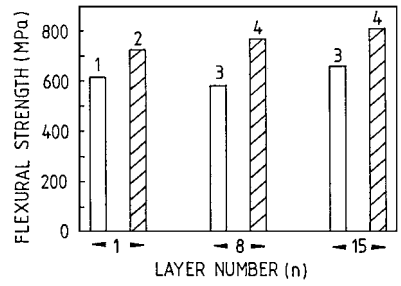

Figure 12 Flexural strength as a function of the number of layers in the crack-free zone for various layer compositions. (1) pure Al_2O_3 tubes, (2) pure PSZ tubes, (3) composite with Al_2O_3 as outer layer, (4) composite with PSZ as outer layer.

much improved through transformation mechanisms. If a/t and $(\alpha_1 - \alpha_2)$ were kept constant and the layer thickness, t, was varied, the model predicted that the critical layer thickness for this system would be 46 μm. In the geometry used in this case, the layer thickness could be changed by changing the number of layers. The critical number of layers was 5.4 (Fig. 10), thus, a 6 layer composite should be crack-free. Extrudates with $n = 3$, 5, 6, 9 and 15 were produced and cracks were clearly visible only in the $n = 3$ samples. However, examining the mechanical data of the specimens (Fig. 11), a significant increase in strength of the tubes can be seen, with the greatest increase being centred around the predicted value of 5.4 layers, indicating a close fit with the prediction. At low layer numbers the strength is very low due to the cracking, while composites above the critical layer number have equal or better strengths than monolithic materials. The higher the layer number the higher is the strength due to crack deflection mechanisms.

The outer layer may either be ZrO_2 or Al_2O_3. Fig. 12 shows that tubes with PSZ as the outer layer are stronger than pure PSZ and tubes with Al_2O_3 on the outside. The Al_2O_3 tubes show similar strength to the composite materials with Al_2O_3 on the outside. This is due to the additional surface stresses developed during formation. In the zirconia outer layer these stresses work to the composite's advantage, as stress induced transformation places the outer layer into compression. There was some evidence that the prediction that a tri-layer composition of $ZrO_2(Y3)/Al_2O_3$, where the total wall

thickness is 250 μm, having zirconia layers either less than 22 or greater than 202 μm would result in crack-free composites (Fig. 8) was upheld in experimental extrudates, but reliable samples for mechanical testing were not produced.

The closer that α_1 can be brought to α_2, the lower the propensity will be for the materials to crack and fail. ZrO_2(Y8) and ZrO_2(Y3) have similar α values. The capability of bringing α_1 and α_2 closer together arises with the formation of composites of Al_2O_3 and ZTA, where despite the difference in toughness the CTE behaviour of the materials is much closer than in the ZrO_2/Al_2O_3 systems discussed earlier. The critical layer thickness for a Al_2O_3/Al_2O_3 (80%) + ZrO_2(Y3) (20%) composite with even layer thickness ($t/d = 0.5$) is 339 μm which implies that cracks should not be found in these composites in the die used in these experiments. No cracks were observed verifying the prediction.

5. Summary

Co-extruded laminated composites may fracture during processing, the cracks forming during the extrusion process itself, during drying, sintering or cooling. Evidence presented in this paper suggests that the major failures occur while cooling from the sintering stage as the materials become less compliant and the different layers exhibit different mechanical properties including thermal contraction. Equations predicting failure on cooling are presented and tested for co-extruded tubes. It is shown that the predictions are valid for a range of zirconia/alumina and ZTA/alumina laminates and that the methods could be used as a predictive tool in composite preparation.

Acknowledgements

The authors wish to thank the ORS scheme and the School of Chemical Engineering for providing the funding for this work. We further acknowledge the support of the EPSRC for the facilities grants.

References

1. P. L. GUTSHALL and G. E. GROSS, *Eng. Fract. Mech.* **1**(2) (1969) 463.
2. W. J. CLEGG, K. KENDALL, N. McN. ALFORD, T. W. BUTTON and J. D. BIRCHALL, *Nature* **347** (1990) 455.
3. W. J. CLEGG, *Materials Science and Technology* **14** (1998) 483.
4. C. J. RUSSO, M. P. HARMER, H. M. CHAN and G. A. MILLER, *J. Amer. Ceram. Soc.* **75**(12) (1992) 3396.
5. D. B. MARSHALL, J. J. RATTO and F. F. LANGE, *ibid.* **74**(12) (1991) 2979.
6. R. LAKSHMINARAYANAN and D. K. SHETTY, *ibid.* **79**(1) (1996) 79.
7. M. OVAICI, M. R. MACKLEY, G. H. McKINLEY and S. J. COOK, *J. Rheol.* **42** (1998) 125.
8. Z. LIANG and S. BLACKBURN, "Proc. Brit. Ceram. Soc., No. 58," edited by J. Binner and J. Yeomans (1998) p. 113.
9. S. HO and Z. G. SUO, *J. Appl. Mech.* **60** (1993) 890.
10. C. HILLMAN, Z. G. SUO and F. F. LANGE, *J. Amer. Ceram. Soc.* **79** (1996) 2127.
11. K. M. LIANG, G. ORANGE and G. J. FANTOZZI, *J. Mater. Sci.* **25** (1990) 207.
12. T. R. WATKINS and D. J. GREEN, *J. Amer. Ceram. Soc.* **77**(3) (1994) 717.
13. K. NIIHARA, A. NAKAHIRA and T. HIRAI, *ibid.* **67** (1984) C-13.
14. N. McN. ALFORD, K. KENDALL, J. D. BIRCHALL, J. H. RAISTRICK and A. J. HOWARD, European Patent EP0183453A2, Filed 15/11/1985.
15. N. McN. ALFORD, J. D. BIRCHALL and K. KENDALL, European Patent EP0288208A2, Filed 14/4/1988.
16. C. VAN HOY, A. BARDA, M. GRIFFITH and J. W. HALLORAN, *J. Amer. Ceram. Soc.* **81**(1) (1998) 152.
17. D. G. A. WHITTEN and J. R. V. BROOKS, "A Dictionary of Geology" (Penguin, 1976).

Received 4 April 2001
and accepted 16 May 2002